

Formulating Superhydrophobic Coatings with Silane for Microfiber Applications

Zh. Suiindik, E. Adotey, N. Kydyrbay, M. Zhazitov, N. Nuraje, O. Toktarbaiuly*

Renewable Energy Laboratory, National Laboratory Astana, Nazarbayev University,
Kabanbay Batyr 53, Astana, Kazakhstan

Article info

Received:
10 February 2024

Received in revised form:
8 April 2024

Accepted:
17 May 2024

Keywords:

Superhydrophobic coatings
Microfiber surfaces
Silica nanoparticles
Polydimethylsiloxane
Water contact angle
pH effects
Textile applications

Abstract

This study investigates the development of superhydrophobic coatings on microfiber surfaces, with a specific focus on cotton, tweed, felt, and polyester fabrics. The resulting coatings demonstrated significant hydrophobicity, with water contact angles ranging from 128.5° for polyester to 148.9° for tweed. In addition, this investigation delves into the influence of pH levels on water contact angles, revealing notable fluctuations; specifically, higher pH levels resulted in decreased contact angles. The results indicated that the tweed fabric had the highest water contact angle at 151.7°, observed at a pH of 4. This study not only underscores the effective hydrophobic performance of these coatings but also highlights their practical applications. In particular, the research demonstrates the potential use of superhydrophobic coatings in the construction of traditional Kazakh ui (yurts), especially emphasizing the promising water repellency properties of felt fibers. Furthermore, this research illustrates a promising approach for producing superhydrophobic coatings on various microfiber surfaces, underlining their extensive potential applications within the textile industry. Overall, the findings suggest that the innovative use of superhydrophobic coatings can significantly enhance the water resistance of traditional and modern fabrics, paving the way for their broader application in various industries, including outdoor textiles and protective clothing.

1. Introduction

Superhydrophobic coatings (SHC) have become popular in many industrial usage due to characteristics such as water repelling, self-cleaning, and anti-icing [1–3]. These coatings are used in a number of fields, including road construction, textiles, oil-water separation, batteries, anti-fouling coatings, and many others [4–6]. The use of hydrophobic materials in construction is a significant application, offering benefits such as enhanced durability, resistance to moisture damage, and improved longevity of building materials [7–11]. As is known, superhydro-

phobic surfaces are usually defined as those with contact angles $>150^\circ$ and rolling angles $<10^\circ$, which provide the above properties and preparation of superhydrophobic coatings based on essential features such as micro-/nanostructure roughness and a low surface energy [12–16].

Superhydrophobic fabrics have emerged as a transformative innovation in material science, offering unparalleled water-repelling capabilities and a myriad of applications across various industries. Inspired by natural phenomena such as the lotus leaf and the water strider, superhydrophobic fabrics mimic these surfaces' ability to repel water droplets with remarkable efficiency [17, 18]. Superhydrophobic surfaces can be generated through two methods: one involves the formation of a rough surface,

*Corresponding author.

E-mail address: olzat.toktarbaiuly@nu.edu.kz

while the other entails altering the current surface using materials possessing low surface energy, such as fluorination or the addition of silicon compounds [19]. One of the most important properties of solid surfaces such as wetting behavior depends on the chemical composition and roughness of surfaces [20]. Surface water repellency can be improved by increasing the roughness of the surface [21, 22]. Fluorochemicals are widely used in textile finishing because of their low surface free energy properties which provide water and oil repellency [23].

Currently, there has been a surge of interest in superhydrophobic fabrics across a wide range of industries. In the field of textiles, these fabrics are being explored for applications such as stain-resistant clothing, waterproof outdoor gear, and breathable yet water-repellent membranes for sportswear. In the biomedical sector, superhydrophobic materials are being investigated for their potential use in medical textiles, implant coatings, oil industry, and drug delivery systems [24–26].

Different studies have been conducted on the production of superhydrophobic, durable, water and oil repellent coatings on different types of textiles. For example, Xue et al. utilized conventional textile finishing techniques to create superhydrophobic surfaces on cotton textiles [27]. They developed a dual-size hierarchical structure by applying a complex coating of silica nanoparticles with functional groups onto microscale cotton fibers that were previously functionalized with epoxy [27]. Xue et al. also documented the creation of water-resistant superhydrophobic poly(ethylene terephthalate) (PET) textiles by blending polydimethylsiloxane and SiO₂ nanoparticles, followed by modification using tetraethoxysilane and cetyl trimethoxysilane under ammonia catalysis through an in situ Stöber reaction [28]. Dimitra et al. developed a coating that generates superhydrophobic or superoleophobic properties, leading to water or oil repellency on silk. Notably, the coating [29] was applied without the need for organic solvents which otherwise could have altered the aesthetic appearance of dyed silk and was easily removed using compressed CO₂. The work of N.A. Ivanova and A.B. Philipchenko introduced a technique for creating superhydrophobic antibacterial textiles for biomedical purposes, employing hydrophobic nanoparticles derived from chitosan [30]. M. Myrzabaeva's study investigates using soot-based hydrophobic sand as an insulator for growing heavy metal-accumulating plants, such as amaranth and sunflower [31]. Z.A. Mansurov et al. synthesize and deposit carbon nanostructures

on silicon and nickel wafers using flame synthesis, pinpointing the best flame locations for maximum hydrophobicity [32].

Most of the studies aforementioned were only directed on superhydrophobic cotton textiles and not on other known fabrics [33–36]. Therefore, this work includes studies on other types of fabrics such as felt, tweed, cotton (medicine and textile) and polyester to show differences in their water repellency properties. Three main groups of fabrics studied in this work, namely natural fiber (cotton), synthetic fiber (polyester) and blended fiber (tweed), which combine both natural and synthetic materials [37]. Our study also shows the superhydrophobic properties of felt fabric, which is commonly used for the construction of Kazakh ui, also so called Kazakh yurts. Various studies have been conducted on architecture, including investigations into the structure of the Kazakh ui [38]. The traditional nomadic shelter of the Kazakh people, called *kiyz ui*, features decorative elements and consists of collapsible lattice and felt fabric structures. The specific type of felt historically used in the Uisk steppes, now located in the modern Altai Mountains region, and has endured to this present day [39]. Given that Kazakh ui serve nomadic functions for the people of Kazakhstan, employing hydrophobic materials for their construction can be viewed as a practical solution.

2. Materials and methods

2.1 Chemicals and microfibers

Silica nanoparticles (Sigma-Aldrich, nanopowder spherical, porous, 5–15 nm particle size (TEM), 99.5% trace metal basis, MW: 60.08 g/mol), Hexadecyltrimethoxysilane (HDTMS) (Sigma-Aldrich, technical, ≥85% (GC). MW: 346.62 g/mol), 1H,1H,2H,2H-Perfluorooctyltriethoxysilane (PFOTS) (Thermo Scientific, 97%), Polydimethylsiloxane trimethylsiloxy (Thermo Scientific, M.W. 4000), Hexane (Sigma-Aldrich, anhydrous, 95%. MW: 86.18 g/mol) were used in all the experiments. NaOH (sodium hydroxide) and HCl (hydrochloric acid) were utilized for different pH solutions. The chemicals were used without further purification. The five different types of microfibers used were cotton, medical cotton, polyester, tweed, and felt. The dimensions of a square shape, 2 cm x 2 cm, was cut from each fiber. The various fabrics were purchased from a chain of local fabric stores.

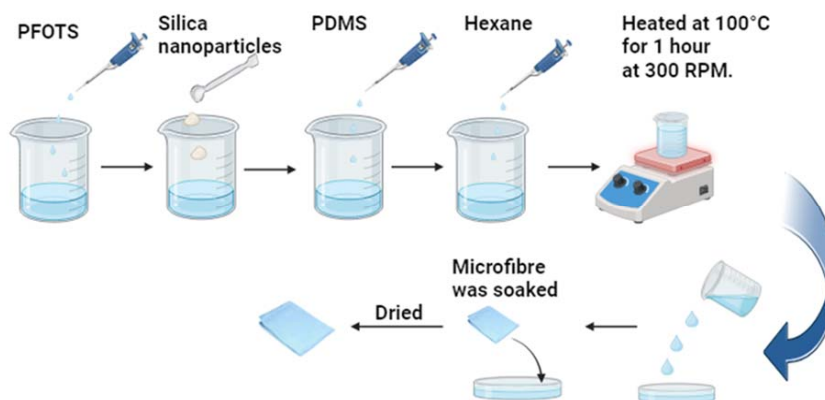


Fig. 1. Preparation of superhydrophobic coatings onto microfiber.

2.2 Preparation of coatings with superhydrophobic properties

Figure 1 illustrates the preparation process of a hydrophobic coating. A homogeneous mixture was prepared by combining commercial silica nanoparticles with HDTMS, with a ratio of 1:4. To this mixture, 150 mL of ethanol was added as a dispersion medium. The mixture was then subjected to mechanical stirring at a speed of 300 rpm for 1 h, at a temperature of 90 °C, to ensure the formation of a colloidal dispersion. The resultant particles were subjected to a centrifugation process for the separation and removal of unreacted materials and by-products. The centrifuged particles were then thoroughly washed with distilled water to remove any residual reactants or impurities. Following the washing step, the particles were transferred to an oven for drying. The ideal drying process was conducted at a temperature of 50 °C and was extended overnight. This step was critical for ensuring the removal of moisture, leading to the formation of superhydrophobic silica particles. The methodology adopted in this experiment was designed to optimize the conditions for the production of superhydrophobic silica particles.

2.3 Fabric pH adjustment and soaking procedure

pH solutions ranging from 2 to 12 were meticulously prepared by adjusting the concentrations of 1M NaOH and 1M HCl through varying amounts of each reagent. Subsequently, fabric samples of identical dimensions 2 cm by 2 cm were individually immersed in containers holding the respective pH solutions. Standardized soaking durations were applied to ensure uniform exposure across samples. After the soaking period, the drying procedure took place overnight at a temperature of 50 °C, ensuring thorough removal of moisture and optimal preservation of the material.

2.4 Impregnation of the fabric materials with the superhydrophobic coating

The approach used to create these coatings, incorporating a blend of silica nanoparticles and a Polydimethylsiloxane, trimethylsiloxy terminated (PDMS). PDMS is a silicon-based organic polymer known for its thermal stability, minimal toxicity, and inherent water-repelling properties. The initial phase of the synthesis involved the preparation of superhydrophobic silica nanoparticles, weighing 0.1 g. To these nanoparticles, 0.2 ml of PFOTS was added. The ratio of silica nanoparticles to PFOTS was meticulously maintained at approximately 1:2. The procedure was continued by incorporating 1 ml of PDMS. Then hexane was added to achieve a PDMS to hexane ratio of 1:30. This ratio was crucial in forming a homogeneous mixture, with the quantity of hexane adjusted based on the desired viscosity of the resultant solution. Given the non-polar nature of PDMS, the solvent selection was pivotal; hexane, a non-polar solvent, was chosen for its proficiency in dissolving PDMS. After the addition of hexane, the mixture was heated at 100 °C for a duration of 1 h, with continuous stirring. This stirring was essential to ensure uniform distribution of nanoparticles and the completion of the reaction. After the heating process, microfiber substrates were immersed in the suspension. Subsequent to the immersion, the coated microfibers were left to dry for 24 h at 60 °C in a drying oven. This drying step is essential for the adhesion and curing of the superhydrophobic coating on the microfiber surfaces.

2.5 Characterization

An FT-IR spectrometer (ANicolet iS10, Thermo Scientific, Waltham, MA, USA) was used to study the formation of silica particles and their modification in

powder form. Contact angles (OCA) of water droplets on the dried fibers were measured by a goniometer (Dataphysics OCA 15 Pro, Filderstadt, Germany). Scanning electron microscopy (SEM) (Zeiss Auriga Crossbeam 540, Carl Zeiss, Oberkochen, Germany) were utilized to investigate the morphology of the dried coatings on the fibers.

3. Results and discussion

Figure 2 illustrates the FTIR characterization of the superhydrophobic coating. The peak observed at 2962.24 cm^{-1} was attributed to the stretching of C-H bonds in CH_3 groups [40], while the band at 1412.35 cm^{-1} was associated with the symmetric stretching vibration of carboxylic groups [41]. Furthermore, the absorption peak at 1257.83 cm^{-1} was assigned to the vibrational and antisymmetric stretching vibration of $-\text{CH}_3$ in $\text{Si}-\text{CH}_3$ [42]. Additionally, the peak at 1009.19 cm^{-1} was identified as corresponding to the $-\text{CH}_3$ rocking vibrational modes [43]. Another observation occurred at 863.93 cm^{-1} , where the bands between 863 cm^{-1} and 872.19 cm^{-1} were interpreted as out-of-plane vibration modes of the carbonate group [44]. Additionally, the peaks observed at 786.26 cm^{-1} were attributed to the presence of Si-C bond stretching [45]. Moreover, the stretching peaks observed at 686.15 cm^{-1} were attributed to $-\text{OH}$ swinging or rocking modes, characteristic of the aliphatic chains [46]. Lastly, the broad absorption bands at 464.21 cm^{-1} were found to correspond to the bending modes of Si-O-Si [47].

Figure 3 shows the scanning electron microscope image of the superhydrophobic precipitate. The image displays the morphology of the particles

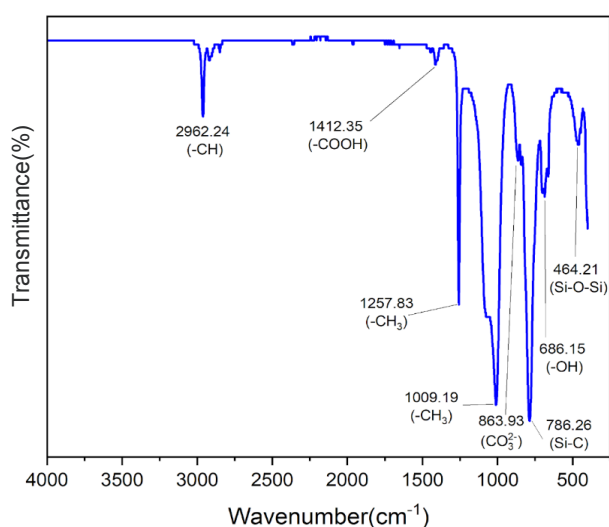


Fig. 2. FTIR characterization of the superhydrophobic coating.

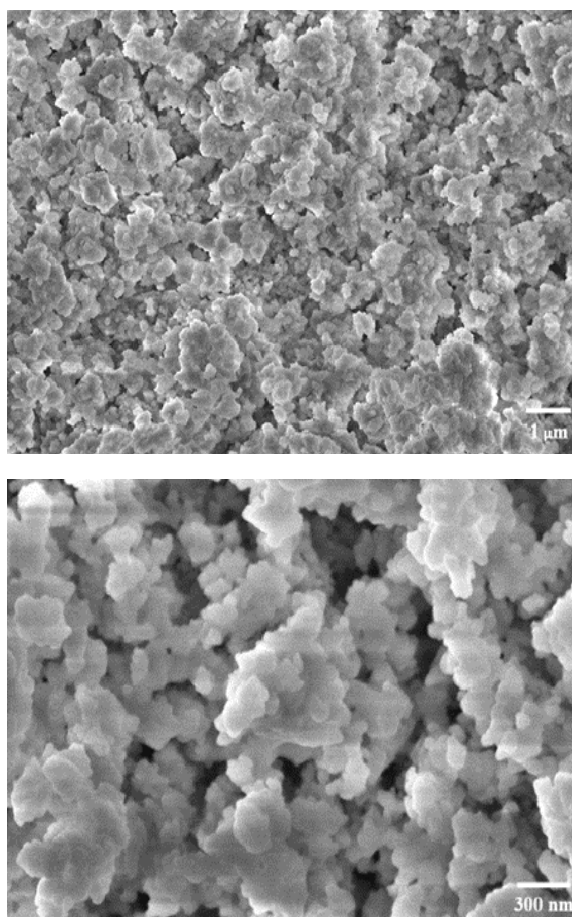


Fig. 3. SEM images revealing the morphology of the particles.

as irregular shapes with agglomeration in the samples. Figure 4 shows the elemental mapping in the sample, and it was evident that fluorine and silicon were uniformly distributed. Figure 5 illustrates the elemental composition of the superhydrophobic precipitate using the Energy Dispersive X-ray Spectroscopy (EDS) spectrum. The spectrum reveals significant peaks, particularly in oxygen (O); 44.54%, silicon (Si); 33.28%, and carbon (C); 21.63%. A minor presence of fluorine (F) is also observed, constituting 0.55% of the composition.

The presence of hydrophobic functional groups such as fluorine (F) groups in polymers contributes to their water-repellent properties. These groups do not interact favorably with water molecules, further enhancing the hydrophobicity of the polymer surface.

Analysis of the EDS spectrum indicates absorption bands ranging from 0.2 to 2 keV, suggesting characteristic elements present in the superhydrophobic coating. The likely sources of these elements such as silicon, oxygen, and carbon are attributed to silica nanoparticles, HDTMS, PFOTS, PDMS, and hexane, while fluoride is associated with PFOTS.

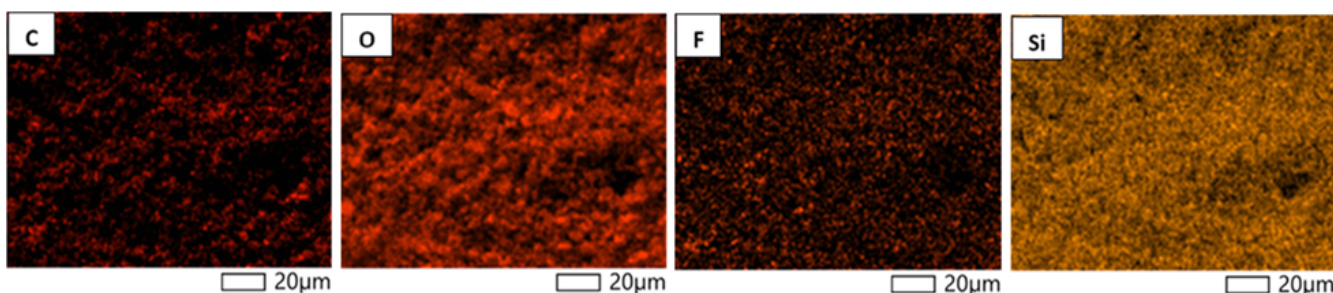


Fig. 4. Elemental mapping of the particles obtained from the EDS analysis.

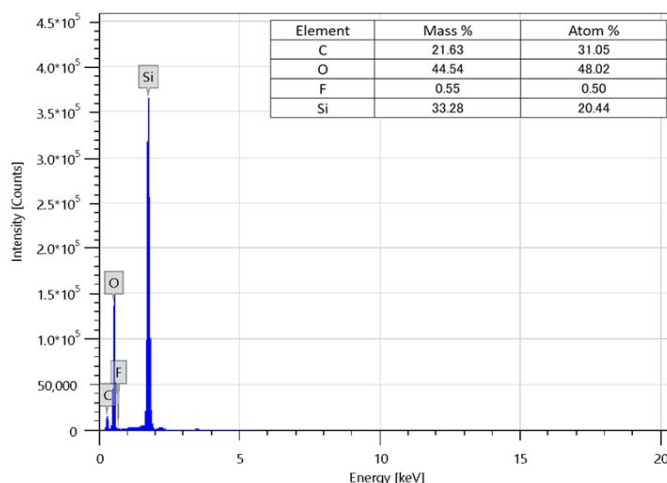


Fig. 5. EDS spectrum and mapping of a Superhydrophobic coating (inserted table shows the fractional contributions of each element).

Figures 6 and 7 show the water contact angle (WCA) of the microfiber samples after a thorough drying process to determine their hydrophobic or hydrophilic nature. The drying process was carried out uniformly across all samples under controlled conditions. A standard sessile drop method was used to measure the WCA, where a calibrated micro-syringe was used to deposit a predetermined volume of distilled water on the microfiber surface. The angle formed at the water-microfiber interface was then measured using a goniometer (OCA 15 EC,

Neurtek Instruments). An amount of 10 μl water droplet was applied to all samples. The WCA with water is crucial for understanding surface wettability. Cotton, medical cotton, polyester, tweed, and felt showed varying degrees of hydrophobicity. Cotton had a CA of 135.0°, medical cotton 141.8°, polyester 128.5°, tweed approximately 148.9°, and felt 138.7°. Generally, tweed demonstrated the highest water contact angle among the tested materials, measuring approximately 148.9°. This exceptionally high contact angle indicates significant hydrophobicity.

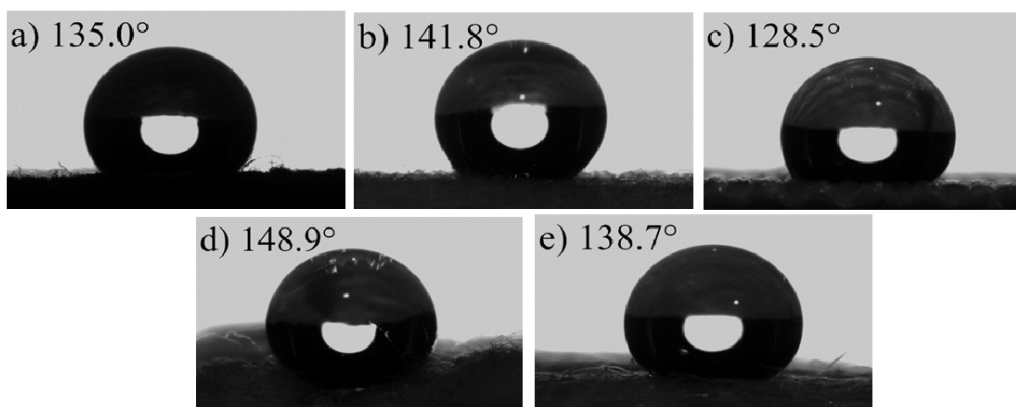


Fig. 6. Water contact angle measurements of a) cotton, b) medical cotton, c) polyester, d) tweed, and e) felt.

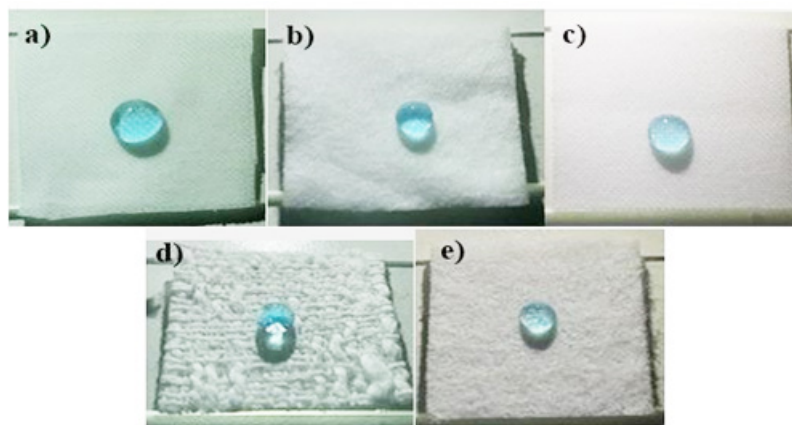


Fig. 7. Demonstration of hydrophobicity of a) cotton, b) medical cotton, c) polyester, d) tweed and e) felt.

Figure 8 shows the results obtained after conducting stretching experiment to investigate the effect of mechanical stretching on the WCA of various fabrics. Through controlled stretching of fabrics, the impact of mechanical deformation on surface characteristics such as roughness, porosity, and surface energy can be investigated, ultimately influencing their interaction with water [48]. After stretching using stable micro systems texture analyzer equipment, the WCA uniformly decreases across all fabrics (Fig. 8). Specifically, cotton's water contact angle decreased by about 4.96%, while medical cotton showed an 8.1% decrease. Polyester experienced the most significant decrease at 17.2%, followed closely by tweed at 15.7%. Felt exhibited a moderate decrease of 9.4%.

Tweed had the highest WCA and thus chemical test was performed solely on it to test any changes to the surface chemistry at different pHs. Different pH solutions were generated by adjusting the concentrations of 1M NaOH and 1M HCl through varying amounts of each reagent. Figure 9 shows the

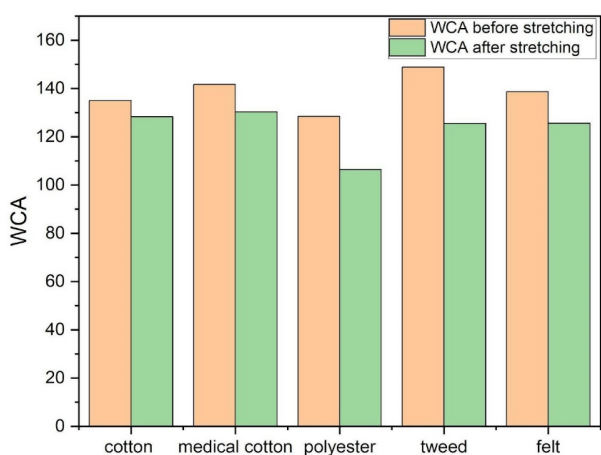


Fig. 8. Water contact angle measurements.

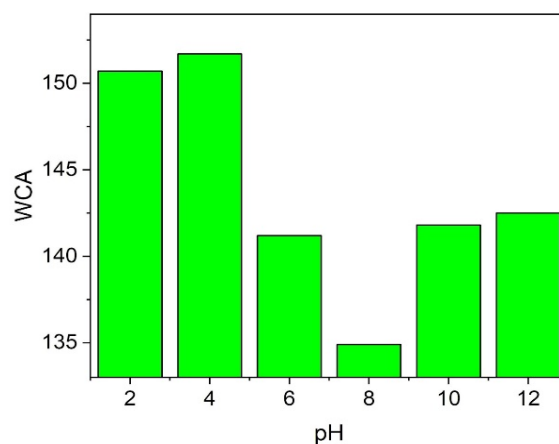


Fig. 9. Water contact angle of the tweed fabric after exposure to various pH solutions.

WCA results obtained for tweed fabric after exposure to solutions with varying pH levels. At pH 2 and 4, the WCA was relatively high, measuring 150.7° and 151.7° , respectively. Subsequently, a decrease in WCA was observed as pH increased, with values of 141.2° and 134.9° recorded at pH 6 and 8, respectively. Notably, a slight increase in WCA was noted at pH 10, measuring 141.8° , and pH 12, measuring 142.5° . By adjusting the pH levels of the solutions and analyzing the resulting WCA investigates how alterations in pH influenced the surface properties of the tweed fabric in particular environments or uses. In general, WCA tends to decrease as pH increases, with some fluctuations in between.

4. Conclusion

This study focuses on developing a superhydrophobic coating on different types of fibers, including cotton, tweed, felt, and polyester, enabling water-repellency properties. Superhydrophobic coatings on microfiber surfaces were prepared using

nanosilica particles and PDMS. This coating, attained via a facile, low-cost, and reliable dip-coating process, illustrates a notable input in the realm of superhydrophobic textile materials. The water contact angle of the coated fibers ranged from 128.5° for polyester to 148.9° for tweed, with tweed exhibiting the highest contact angle and wettability, leading to its selection for further investigation involving exposure to various pH solutions. At a pH level of 4, tweed material exhibits the highest WCA, measuring approximately 151.7°. The superhydrophobic coated felt fibers, intended for incorporation into the construction of traditional Kazakh ui, have demonstrated good water repellency, evidenced by a WCA of 138.7°. Despite tweed exhibiting the highest WCA, it's pertinent to acknowledge that felt fiber serves as the predominant material utilized in Kazakh ui.

Acknowledgments

The authors would like to acknowledge the support of the Ministry of Science and Higher Education of the Republic of Kazakhstan under Grant No. AP19679222. They acknowledge the assistance from the Targeted Program of the MHES of the Republic of Kazakhstan, Grant No. BR21882439.

References

- [1]. A. Kurbanova, N. Myrzakhmetova, N. Akimbayeva, K. Kishibayev, et al., *Coatings* 12 (2022) 1422. DOI: [10.3390/coatings12101422](https://doi.org/10.3390/coatings12101422)
- [2]. O. Toktarbaiuly, A. Kurbanova, G. Imekova, M. Abutalip, Zh. Toktarbay, *Eurasian Chem.-Technol. J.* 25 (2023) 193–200. DOI: [10.18321/ectj1522](https://doi.org/10.18321/ectj1522)
- [3]. A. Seralin, G. Sugurbekova, A. Kurbanova, N. Nuraje, O. Toktarbaiuly, *Eurasian Chem.-Technol. J.* 24 (2022) 251–258. DOI: [10.18321/ectj1438](https://doi.org/10.18321/ectj1438)
- [4]. M. Balaish, J. Jung, I. Kim, Y. Ein-Eli, *Adv. Funct. Mater.* 30 (2019). DOI: [10.1002/adfm.201808303](https://doi.org/10.1002/adfm.201808303)
- [5]. A. Hooda, M.S. Goyat, J.K. Pandey, A. Kumar, R. Gupta, *Prog. Org. Coat.* 142 (2020) 105557. DOI: [10.1016/j.porgcoat.2020.105557](https://doi.org/10.1016/j.porgcoat.2020.105557)
- [6]. K. Manoharan, S. Bhattacharya, *Journal of Micromanufacturing* 2 (2019) 59–78. DOI: [10.1177/2516598419836345](https://doi.org/10.1177/2516598419836345)
- [7]. M.J. Al-Kheetan, M.M. Rahman, D.A. Chamberlain, *J. Mater. Civ. Eng.* 31 (2019). DOI: [10.1061/\(ASCE\)MT.1943-5533.0002694](https://doi.org/10.1061/(ASCE)MT.1943-5533.0002694)
- [8]. M.J. Al-Kheetan, M.M. Rahman, D.A. Chamberlain, *Int. J. Build. Pathol. Adapt.* 36 (2018) 77–92. DOI: [10.1108/IJBPA-02-2017-0011](https://doi.org/10.1108/IJBPA-02-2017-0011)
- [9]. F.W. Al-Awabdeh, M.J. Al-Kheetan, Y.S. Jweihan, H. Al-Hamaiedeh, S.H. Ghaffar, *Results Eng.* 16 (2022) 100790. DOI: [10.1016/j.rineng.2022.100790](https://doi.org/10.1016/j.rineng.2022.100790)
- [10]. M.J. Al-Kheetan, J. Byzyka, S.H. Ghaffar, *Sustainability* 13 (2021) 4949. DOI: [10.3390/su13094949](https://doi.org/10.3390/su13094949)
- [11]. M.J. Al-Kheetan, M. Al-Tarawneh, S.H. Ghaffar, M. Chougan, et al., *Struct. Concr.* 22 (2021) E1050–E1061. DOI: [10.1002/suco.202000214](https://doi.org/10.1002/suco.202000214)
- [12]. H.Y. Erbil, *Langmuir* 36 (2020) 2493–2509. DOI: [10.1021/acs.langmuir.9b03908](https://doi.org/10.1021/acs.langmuir.9b03908)
- [13]. C. Yang, Q. Zeng, J. Huang, Z. Guo, *Adv. Colloid Interface Sci.* 306 (2022) 102724. DOI: [10.1016/j.cis.2022.102724](https://doi.org/10.1016/j.cis.2022.102724)
- [14]. M. He, Q. Zhang, X. Zeng, D. Cui, et al., *Adv. Mater.* 25 (2013) 2291–2295. DOI: [10.1002/adma.201204660](https://doi.org/10.1002/adma.201204660)
- [15]. Y. Hou, Z. Wang, J. Guo, H. Shen, et al., *J. Mater. Chem. A* 3 (2015) 23252–23260. DOI: [10.1039/C5TA05612H](https://doi.org/10.1039/C5TA05612H)
- [16]. Y. Li, S. Chen, M. Wu, J. Sun, *Adv. Mater.* 26 (2014) 3344–3348. DOI: [10.1002/adma.201306136](https://doi.org/10.1002/adma.201306136)
- [17]. F. Su, K. Yao, *ACS Appl. Mater. Interfaces* 6 (2014) 8762–8770. DOI: [10.1021/am501539b](https://doi.org/10.1021/am501539b)
- [18]. B. Bhushan, *Philos. Trans. R. Soc. A* 367 (2009) 1445–1486. DOI: [10.1098/rsta.2009.0011](https://doi.org/10.1098/rsta.2009.0011)
- [19]. L. Feng, S. Li, H. Li, J. Zhai, et al., *Angew. Chem. Int. Ed.* 41 (2002) 1221–1223. DOI: [10.1002/1521-3773\(20020402\)41:7<1221::AID-ANIE1221>3.0.CO;2-G](https://doi.org/10.1002/1521-3773(20020402)41:7<1221::AID-ANIE1221>3.0.CO;2-G)
- [20]. H. Gau, S. Herminghaus, P. Lenz, R. Lipowsky, *Science* 283 (1999) 46. DOI: [10.1126/science.283.5398.46](https://doi.org/10.1126/science.283.5398.46)
- [21]. W. Chen, Y. Fadeev, M.C. Heieh, D. Oner, Jet al., *Langmuir* 15 (1999) 3395–3399. DOI: [10.1021/la990074s](https://doi.org/10.1021/la990074s)
- [22]. A. Nakajima, A. Fujishima, K. Hashimoto, T. Watanabe, *Adv. Mater.* 11 (1999) 1365. DOI: [10.1002/\(SICI\)1521-4095\(199911\)11:16<1365::AID-ADMA1365>3.0.CO;2-F](https://doi.org/10.1002/(SICI)1521-4095(199911)11:16<1365::AID-ADMA1365>3.0.CO;2-F)
- [23]. L. Amado, S. Mireia, B. Miren, V. Karnele, M. Antxon, *Prog. Org. Coat.* 150 (2021) 105968. DOI: [10.1016/j.porgcoat.2020.105968](https://doi.org/10.1016/j.porgcoat.2020.105968)
- [24]. Sri A. Kavitha, P. Deeksha, G. Deepika G. et. al., *J. Ind. Eng. Chem.* 92 (2020) 1–17. DOI: [10.1016/j.jiec.2020.08.008](https://doi.org/10.1016/j.jiec.2020.08.008)
- [25]. R. Kumar, A. Kumar Sahani, *Mater. Today: Proc.* 45 (2021) 5655–5659. DOI: [10.1016/j.matpr.2021.02.457](https://doi.org/10.1016/j.matpr.2021.02.457)
- [26]. X. Zhao, M. Abutalip, Kh. Afroz, N. Nuraje, *Langmuir* 35 (2019) 1606–1612. DOI: [10.1021/acs.langmuir.8b03561](https://doi.org/10.1021/acs.langmuir.8b03561)
- [27]. Ch. Xue, Sh. Jia, J. Zhang, L. Tian, *Thin Solid Films* 517 (2009) 4593–4598. DOI: [10.1016/j.tsf.2009.03.185](https://doi.org/10.1016/j.tsf.2009.03.185)
- [28]. Ch. Xue, M. Li, X. Guo, Q. An, Sh. Jia, *Surf. Coat. Tech.* 310 (2017) 134–142. DOI: [10.1016/j.surfcoat.2016.12.049](https://doi.org/10.1016/j.surfcoat.2016.12.049)

- [29]. D. Aslanidou, I. Karapanagiotis, C. Panayiotou, *Prog. Org. Coat.* 97 (2016) 44–52. DOI: [10.1016/j.porgcoat.2016.03.013](https://doi.org/10.1016/j.porgcoat.2016.03.013)
- [30]. N.A. Ivanova, A.B. Philipchenko, *Appl. Surf. Sci.* 263 (2012) 783–787. DOI: [10.1016/j.apsusc.2012.09.173](https://doi.org/10.1016/j.apsusc.2012.09.173)
- [31]. M. Myrzabaeva, Z. Insepov, K.K. Boguspaev, D.G. Faleev, et al., *Eurasian Chem.-Technol. J.* 19 (2017) 91–98. DOI: [10.18321/ectj507](https://doi.org/10.18321/ectj507)
- [32]. Z.A. Mansurov, M. Nazhipkyzy, B.T. Lesbayev, N.G. Prikhodko, et al., *Eurasian Chem.-Technol. J.* 14 (2012) 19–23. DOI: [10.18321/ectj94](https://doi.org/10.18321/ectj94)
- [33]. B. Deng, R. Cai, Y. Yu, H. Jiang, et al., *Adv. Mater.* 22 (2010) 5473–5477. DOI: [10.1002/adma.201002614](https://doi.org/10.1002/adma.201002614)
- [34]. Ch. Xue, Sh. Jia, J. Zhang, L. Tian, et al., *Sci. Technol. Adv. Mater.* 9 (2008) 035008. DOI: [10.1088/1468-6996/9/3/035008](https://doi.org/10.1088/1468-6996/9/3/035008)
- [35]. M.Sh. Khalil-Abad, M.E. Yazdanshenas, *J. Colloid Interface Sci.* 351 (2010) 293–298. DOI: [10.1016/j.jcis.2010.07.049](https://doi.org/10.1016/j.jcis.2010.07.049)
- [36]. X. Zhou, Zh. Zhang, X. Xu, F. Guo, et al., *ACS Appl. Mater. Interfaces* 5 (2013) 7208–7214. DOI: [10.1021/am4015346](https://doi.org/10.1021/am4015346)
- [37]. GfG (2024) Types of fabric-different kinds of natural & synthetic fibres, GeeksforGeeks. Available at: <https://www.geeksforgeeks.org/types-of-fabric/> (Accessed: 15 March 2024).
- [38]. Y.Y. Lichman, T.M. Doroschenko, *European Journal of Science and Theology* 12 (2016) 221–232.
- [39]. E.V. Chenchulaeva, I.V. Kulikova, *Vestnik Tomskogo gosudarstvennogo arkhitekturno-stroitel'nogo universiteta* [Journal of Construction and Architecture] 24 (2022) 39–50. (In Russ.) DOI: [10.31675/1607-1859-2022-24-2-39-5032](https://doi.org/10.31675/1607-1859-2022-24-2-39-5032)
- [40]. S.C. Eluu, J.D. Obayemi, A.A. Salifu, D. Yiporo, et al., *Sci. Rep.* 14 (2024) 31. DOI: [10.1038/s41598-023-50656-6](https://doi.org/10.1038/s41598-023-50656-6)
- [41]. P. Ezati, J.-W. Rhim, M. Moradi, H. Tajik, R. Molaei, *Carbohydr. Polym.* 246 (2020). DOI: [10.1016/j.carbpol.2020.116614](https://doi.org/10.1016/j.carbpol.2020.116614)
- [42]. Y. Chen, J. Li, Y. Hong, W. He, et al., *J. Mater. Sci.: Mater. Electron.* 34 (2023) 1600. DOI: [10.1007/s10854-023-10966-x](https://doi.org/10.1007/s10854-023-10966-x)
- [43]. M. Baibarac, A. Nila, I. Smaranda, M. Stroe, et al., *Materials* 14 (2021) 753. DOI: [10.3390/ma14040753](https://doi.org/10.3390/ma14040753)
- [44]. K.Oyedeko, O.Akinyemi, O.Ogunyemi, S.A.Olaleru, et al., *J. Appl. Res. Technol.* 21 (2023) 945–951. DOI: [10.22201/icat.24486736e.2023.21.6.2153](https://doi.org/10.22201/icat.24486736e.2023.21.6.2153)
- [45]. M. Aurilio, H. Baaj. Examining the Effects of a Self-healing Elastomer on the Properties of Bitumen. In book: Proceedings of the RILEM International Symposium on Bituminous Materials, 2022. DOI: [10.1007/978-3-030-46455-4_109](https://doi.org/10.1007/978-3-030-46455-4_109)
- [46]. M.K. Trivedi, R.M. Tallapragada, A. Branton, D. Trivedi, et al., *J. Fundam. Renewable Energy Appl.* 5 (2015). DOI: [10.4172/2090-4541.1000180](https://doi.org/10.4172/2090-4541.1000180)
- [47]. S. Abdulgafar, Y. Hassan, M. Ibrahim, *J. Mater. Sci.: Mater. Electron.* 34 (2023) 979. DOI: [10.1007/s10854-023-10436-4](https://doi.org/10.1007/s10854-023-10436-4)
- [48]. M. Nueraji, Z. Toktarbay, A. Ardakkyzy, D. Sridhar, et al., *Environ. Res.* 220 (2023) 115212. DOI: [10.1016/j.envres.2023.115212](https://doi.org/10.1016/j.envres.2023.115212)